



Monolithic full-color microdisplay using patterned quantum dot photoresist on dual-wavelength LED epilayers

Peian Li | Xu Zhang SID Member | Yangfeng Li | Longheng Qi | Chak Wah Tang | Kei May Lau

Department of Electronic and Computer Engineering, Hong Kong University of Science and Technology, Hong Kong

Correspondence

Kei May Lau, Department of Electronic and Computer Engineering, Hong Kong University of Science and Technology, Clear Water Bay, Hong Kong.
Email: eekmlau@ust.hk

Funding information

Innovation and Technology Support Program of Hong Kong, Grant/Award Number: ITS/382/17FP

Abstract

A passive-matrix monolithic full-color InGaN light emitting diode (LED) microdisplay with 40×40 full-color pixels is demonstrated. Each full-color pixel consists of red, green, and blue (RGB) subpixels that have a pitch size of $40 \mu\text{m} \times 120 \mu\text{m}$. The full-color microdisplay is monolithically fabricated on blue/green dual-wavelength LED epilayers, using red quantum dot photoresist as a color converter. Pure RGB emission and a wide color gamut are achieved, as shown by electroluminescence spectra. Full-color patterns with controllable grayscale and color mixing can be clearly rendered driven by a full-color microdisplay controller, indicating tremendous potential of this novel approach for full-color LED microdisplays in the future.

KEY WORDS

full-color, LED, microdisplay, quantum dot

1 | INTRODUCTION

Microdisplays are highly attractive to researchers and engineers nowadays because they are widely used in near-eye display technologies and wearable electronics.¹ Traditional microdisplays are based on well-established liquid crystal display (LCD)² or organic light emitting diode (OLED)³ display technologies. Compared to traditional displays, light emitting diode (LED) microdisplays offer higher brightness, better outdoor performance, superior stability, and longer lifetime.⁴ Nevertheless, production-friendly approaches for full-color LED microdisplays have not been developed yet. The major reason is that red, green, and blue (RGB) LEDs are generally made from different starting epiwafers, with distinct device structures.⁴ Thus, manufacturing processes to achieve full-color emission on the same display panel are complex and challenging.

Extensive efforts have been made in developing mass-transfer technologies for full-color LED microdisplays.⁵ In this approach, fabricated InGaN blue/green and AlGaInP red LED pixels are transferred from independent processed

epiwafers to the same display panel pixel by pixel. The pick-and-place transfer process is effective for large LED pixels, but inherent yield and cost issues arise as the pixel size scales down to the micron range. Monolithic fabrication, with RGB subpixels directly fabricated at the wafer level on the same display panel, is thus preferred for high resolution microdisplays. Several monolithic approaches, including works using molecular beam epitaxy (MBE) growth of InGaN nanowires,^{6,7} strain-induced wavelength shift,^{8–10} wafer stacking,^{11,12} and epi-layer adhesive bonding,^{13,14} have been discussed. However, simple and reliable methods have yet to be demonstrated for high yield production of full-color LED microdisplays to date.

Color conversion technology using colloidal quantum dots (QDs), with monochromatic micro-LED arrays as the pump source, provides another monolithic method for full-color LED microdisplays.^{5,15} Colloidal QDs are superior to other phosphors because of their higher quantum yield, broad absorption spectrum, and narrow emission peak. In addition, the emission wavelength of QDs can cover an ultrawide color gamut by controlling the

synthesized QD size.⁴ However, the effectiveness of QD color conversion is still under investigation. In previous studies, researchers patterned RGB QDs on a UV-A LED microdisplay by aerosol jet printing for full-color realization,^{16,17} but the printed QD layer was too thin for sufficient UV absorption. The aerosol jet printing also had a limited linewidth of about 30–40 μm,¹⁷ which can be hardly applicable in fine pitch pixel patterning. A photolithography-based lift-off process was demonstrated to achieve finer QD patterns, but the deposited layer was tens-of-nanometers-thick QD aggregation. It was intended to work for self-emissive QD devices but could not be applied as a color converter.^{18,19}

QD photoresist has also been investigated as a color converter because of its controllable thickness, homogenous dispersion of QDs, and fine patterning capability.^{20,21} Research on the morphology and photoluminescence (PL) of QD photoresist suggests that it is a potential candidate for full-color LED microdisplay applications.²² Thus, QD photoresist has been adopted in our work. However, patterning QD photoresists with distinct primary colors on monochromatic blue or UV LED microdisplays complicates the process. Moreover, the luminance of the converted light is limited by the QD conversion efficiency, especially for the green QD which has much worse performance compared with the red QD. Therefore, using high-brightness green InGaN LEDs instead of green QD is more competitive. Some studies on green/blue LED integration^{14,23,24} demonstrate that growth of blue/green dual-wavelength InGaN LEDs is feasible. The QD photoresist color conversion process can be greatly simplified, and the luminance can be further improved if high-brightness dual-wavelength LEDs are used.

We have developed a novel fabrication approach for a passive-matrix monolithic full-color InGaN LED microdisplay. In this approach, blue/green dual-wavelength LED epilayers are grown on a sapphire substrate and then monolithically fabricated to form an LED array with blue/green dual-wavelength emission. Blue and green subpixels can be easily defined by coating blue and green color filters (CFs) onto different subpixels, respectively. Red subpixels are demonstrated using red QD photoresist patterned on the top of subpixels to convert the original blue/green light emission into red. A red CF is also adopted for the red subpixels to eliminate unabsorbed blue/green light. A relatively wide color gamut is achieved by this novel technology with potential high yield.

2 | EXPERIMENT DESCRIPTION

Blue/green dual-wavelength epilayers were grown on a 2-inch (0001) sapphire substrate by metal-organic

chemical vapor deposition (MOCVD). Both green and blue quantum wells (QWs) were sequentially grown in the same active region based on our previous research.²³ The epistructure features a single active region, different from dual-wavelength LEDs involving a tunnel junction structure²⁴ which may lead to very high forward voltages. Our dual-wavelength LED structure (Figure 1A) consists of a 0.5-μm undoped-GaN layer, a 3.0-μm n-GaN contact layer, strain compensation shallow wells, 3 × blue QWs, 1 × green QW, 1 × blue QW, an electron blocking layer, and a 200 nm p-GaN layer grown in sequence. The green QW was deliberately grown between one blue QW on top and three blue QWs on the bottom. Theoretically, the QW near p-GaN has more significant carrier injection.^{25,26} Thus, the emission of this dual-wavelength LED is dominated by the top blue QW, whereas the carrier injection into the green QW is limited.

Blue-dominant emission is preferred in this work. On the one hand, higher red QD conversion efficiency can be achieved pumped by blue light, whereas on the other, the luminous intensity of the green subpixels will not be too strong, resulting in easier balancing of the luminance from the RGB subpixels while maintaining a similar driving current. The electroluminescence (EL) spectra were calibrated on a large circular mesa-structure LED (Figure 1B) using an integration sphere. The non-uniformity brightness of the LED was caused by current spreading issue and the nonuniform QW growth, limited by our experiment facilities. Well-separated, blue-dominant dual-wavelength emission can be clearly observed in Figure 1C at all the injection currents. The blue and green peaks are located at 460 and 539 nm at 20 mA, and the full width at half maximum (FWHM) of the peaks are 24 and 35 nm, respectively. The light output power (LOP) is 2.20 mW with 20 mA current injection, where the power of blue peak (400–500 nm) is 1.25 mW and that of green peak (500–600 nm) is 0.95 mW. Strong green light emission from the III-nitride is generated without the need of color conversion procedure. Although the efficiency of the blue QWs in the dual-wavelength LEDs is lower than that of conventional single-wavelength blue LEDs, the blue light emission is sufficiently strong for LED microdisplays.

The designed dimensions of our passive-matrix monolithic full-color microdisplay panel are 10.966 mm × 7.850 mm. The display panel contains 40 × 40 full-color pixels with a 120 μm × 120 μm pixel pitch. Each full-color pixel has three RGB rectangular subpixels with pitch size of 40 μm × 120 μm. Figure 2A gives the layout of the display panel and peripheral bonding pads. Figure 2B illustrates the plane view of the pixel design. The LED subpixel array has a typical mesa structure with isolation trenches between subpixels. The

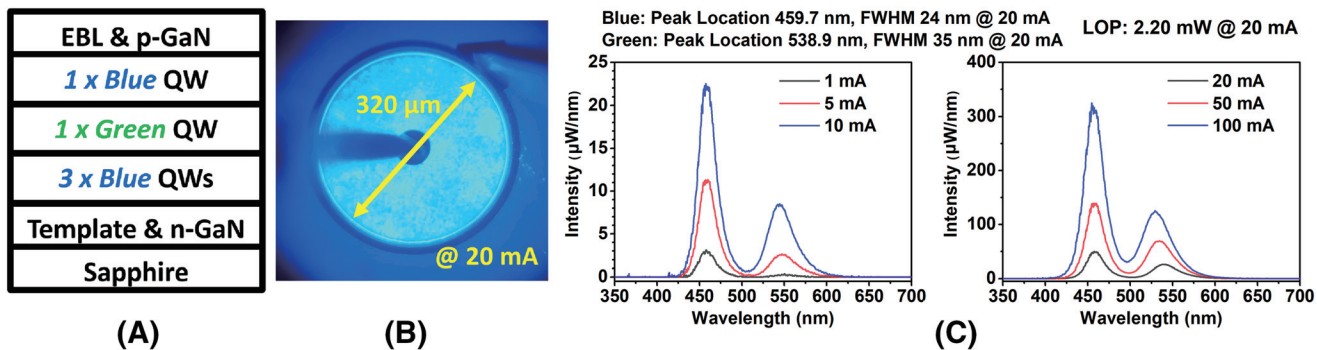
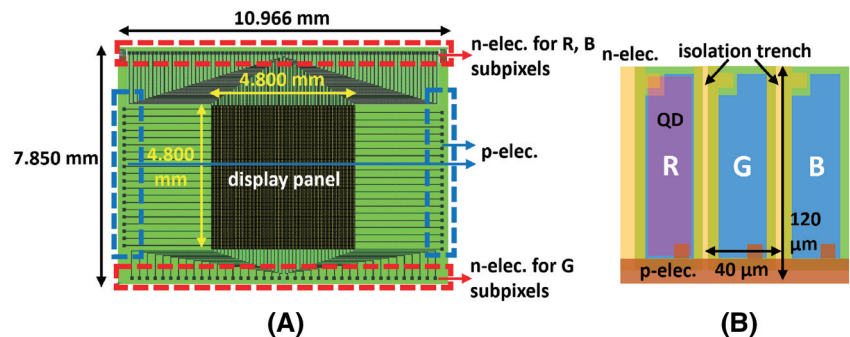


FIGURE 1 (A) Structure of dual-wavelength LED epi-wafers. (B) A 320- μm -diameter circular LED testing device. (C) EL spectra at different injection currents of the testing device

FIGURE 2 (A) Layout and dimensions of the full-color microdisplay. (B) Schematic plane view of a full-color pixel



subpixels share common cathodes in each column and common anodes in each row. QD photoresist film is patterned on the red subpixels for color conversion. RGB CFs cover the top of the subpixels to filter most of the undesired light components. Red CF is also applied as a filling into the pixel isolation trenches and a light absorbing layer at the backside of the display panel to attenuate optical crosstalk.

The remainder of this section describes the fabrication process of the full-color microdisplay. A 1- μm -thick SiO_2 layer was deposited by plasma enhanced chemical vapor deposition (PECVD) and patterned as a hard mask. Then the isolation trenches were etched by BCl_3/Cl_2 -based inductive coupled plasma (ICP) etching. A 115-nm indium tin oxide (ITO) current spreading layer was deposited on p-GaN by e-beam evaporation and patterned in diluted aqua regia using high-temperature photoresist as a mask. After the ITO layer patterning, the photoresist was reused as the mask for 1- μm -deep LED subpixel mesa formation by BCl_3/Cl_2 ICP etching. This self-aligned process prevented any possible misalignment between the ITO layer and mesas. Afterwards, the ITO layer was annealed to form ohmic contact with the p-GaN. The structure and inspection pictures after pixel formation are illustrated in Figure 3A.

After the annealing process, the red CF was filled into the isolation trenches to reduce optical crosstalk. EOC, a

commercial product of highly transparent negative overcoat photoresist, was coated as a passivation and planarization layer covering all subpixels, with opening vias in the electrode contact areas. In addition, a special opening was designed on top of the red subpixels to form cavities for the QD photoresist accumulation. Cathode electrodes ($\text{Ti}/\text{Al}/\text{Ti}/\text{Au}$, 20/240/50/50 nm) were deposited on the EOC layer and connected with n-GaN through the EOC opening vias. The second EOC passivation layer for n/p electrodes insulation was coated in a similar way. The 3- μm -thick Ti/Cu-based anode electrodes were deposited for the p-GaN connection in each row using thick photoresist ($\sim 10 \mu\text{m}$) as the lift-off mask. The structure and inspection pictures after electrode deposition are illustrated in Figure 3B.

Next, blue and green CFs were coated and patterned on corresponding blue and green subpixels. To form the red subpixels, red QD photoresist was synthesized and patterned as a color conversion layer. The QD pristine solution was dispersed in the EOC at the volume ratio of 1: 2 (QD: EOC) to realize the QD photoresist. Red CdSe/ZnS colloidal QDs emitting at 630 nm were provided by our collaborators. The QDs had a concentration of 150 mg/ml dispersed in toluene. Before photolithography, the QD photoresist was soft baked at 50°C to prevent QD degradation under high temperature in the atmosphere. The QD photoresist was exposed under a

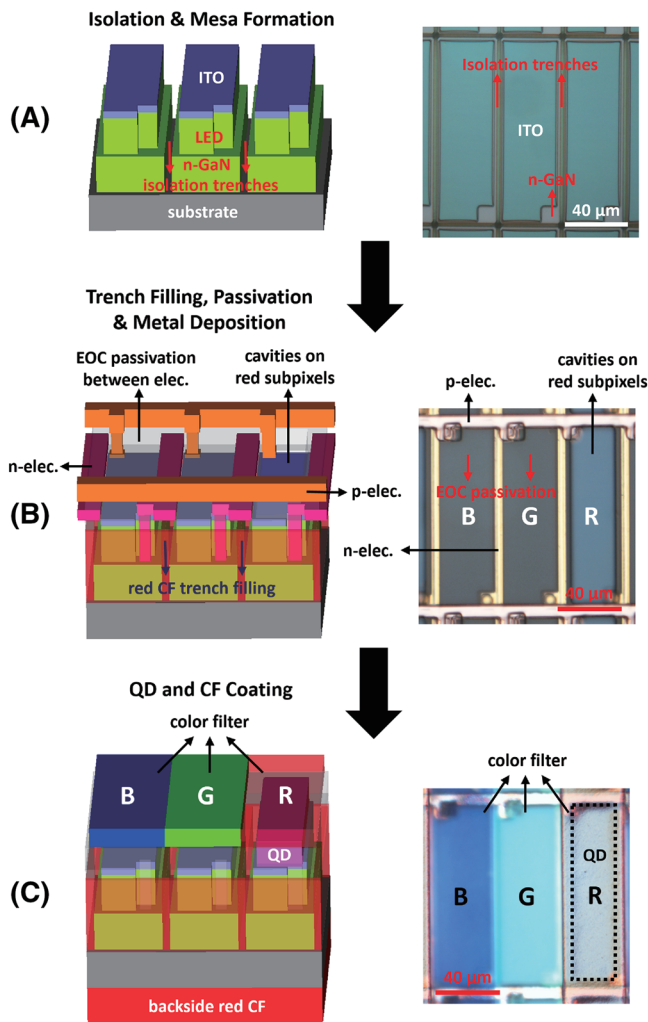


FIGURE 3 Fabrication process of full-color microdisplay. (A) Pixel formation. (B) Electrodes deposition. (C) QD and CF coating

dose of 580 mJ/cm^2 (for a $3.5\text{-}\mu\text{m}$ -thick layer) and developed in a KOH-based developer. Only the QD photoresist in the EOC cavities on the red subpixels remained after developing. Because the QD only absorbed part of the pump light, red CF was coated to cover the QD layer to filter most of the remaining blue/green light. The polished backside of the sapphire substrate was also coated with a thick red CF ($>10 \mu\text{m}$) for elimination of light channeling in the underlying substrate. The completed structure and inspection pictures are illustrated in Figure 3C.

3 | CHARACTERIZATION AND DISCUSSION

An inspection picture of the QD photoresist patterns is shown in Figure 4A. The QD photoresist patterns are

semitransparent, and the gray color is caused by light scattering of the partially aggregated QDs. The fluorescence image in Figure 4B proves that the QD film has strong and uniform fluorescence emissive intensity. The thickness of the QDs was measured by a profiler, as shown in Figure 4C. The EOC opening on the red subpixel not only facilitates the QD film accumulation but also partially compensates the height difference between the thick QD patterns and the thin blue/green CF layers. Therefore, it leads to a conformal coverage and uniform thickness when coating the red CF. The depth of the cavities formed during patterning two EOC layers is about $2.5 \mu\text{m}$ (Figure 4C black line). The patterned QD layer is merely $1 \mu\text{m}$ over the CF layers to reach a total thickness of $3.5 \mu\text{m}$ (Figure 4C red line), which is level enough for the red CF coverage.

The EL performance of a single red subpixel after QD patterning is plotted in Figure 4D. The QD-converted output power accounts for 21.4% of the total LOP in the dual-wavelength LEDs, calculated by integrating the spectral power distribution of the red peak (from 580 to 750 nm). Such performance can be attributed to the enhancement of Mie scattering by the partially aggregated QDs, provided that the particle size is comparable to the wavelength of visible light.²⁷ The scattering phenomenon increases the length of the optical path, thus enhancing the absorption of the excitation light and improving the conversion efficiency. High conversion efficiency requires crucial optimization in the concentration of QD dispersion to prevent excessive aggregation, and the protection ligands of QDs need to be carefully chosen so as to maintain the stability of QDs in the QD photoresist.²⁸

Color conversion properties of a $2\text{-}\mu\text{m}$ -thick QD layer were estimated on large ($320\text{-}\mu\text{m}$ -diameter) conventional single-wavelength blue (440 nm) or green (520 nm) LEDs at 20-mA injection current, with results listed in Table 1. The original pump LOP was firstly measured before QD photoresist coating. The red LOP (integrated from 580 to 750 nm) and the pump LOP (not absorbed by QDs) were then measured after QD photoresist coating. The absorbed pump LOP was determined by the difference of the pump LOP before and after QD coating. The calculated conversion efficiencies (red LOP/absorbed pump LOP) of the blue (33.87%) and the green (36.08%) are comparable with results in the other work.²⁰ Compared with green photons, blue photons have much higher energy than red photons. In the QD photon conversion, there is more energy loss for the blue pump light. Consequently, the conversion efficiency of green pump light, calculated from optical power, has a slightly higher result. However, the percentage of LOP absorbed (absorbed pump LOP/original pump LOP) of the blue

FIGURE 4 (A) Photo of QD photoresist patterns on red subpixels. (B) Fluorescence image of QD photoresist patterns. (C) Profile of RGB subpixels before and after QD patterning, measured by a profilometer. (D) EL spectrum of the red subpixel after QD patterning

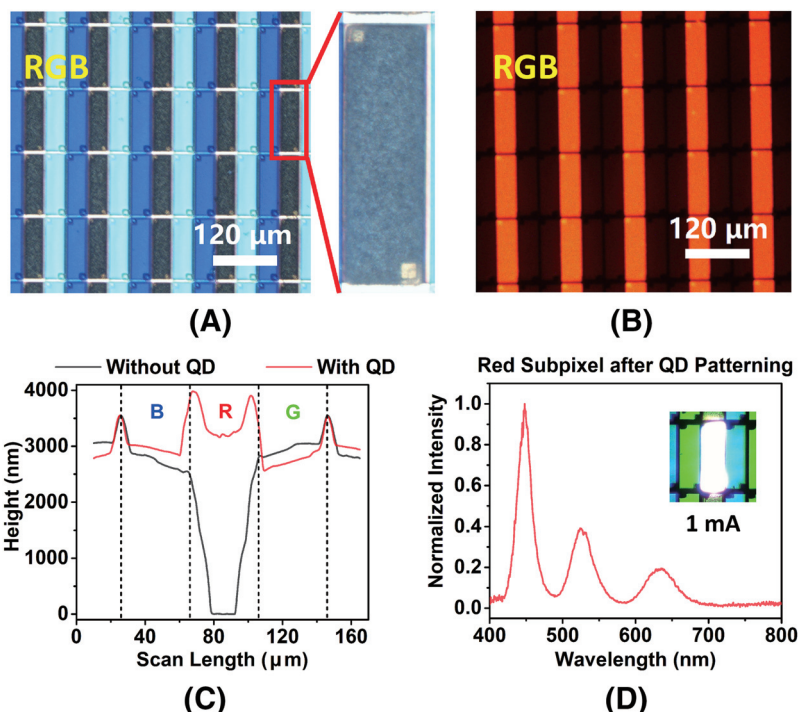


TABLE 1 Estimation of light conversion efficiency of a 2-μm-thick QD photoresist layer (measured at 20 mA)

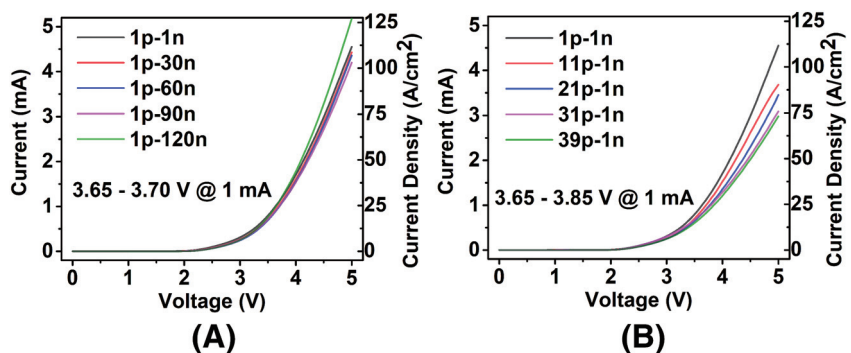
Samples	Conversion Efficiency (Red LOP/Absorbed Pump LOP, %)	Percentage of LOP Absorbed (Absorbed Pump LOP/Original Pump LOP, %)	Overall Efficiency (Red LOP/Original Pump LOP, %)
440 nm blue LED	33.87	66.84	22.67
520 nm green LED	36.08	28.08	10.13

pump light is higher than the green. As a result, the overall efficiency (red LOP/original pump LOP) of the green is less than the blue. The issue of limited green light absorption is not severe for the full-color microdisplay because the dual-wavelength LEDs pumping the QD photoresist are blue-dominant.

The I-V characteristics of the subpixels are illustrated in Figure 5A,B. The electrodes are labeled from

1n to 120n (n-electrodes, from left to right) and from 1p to 40p (p-electrodes, from top to bottom). Figure 5 indicates that the forward voltage was uniform, around 3.65–3.70 V along the same p-electrodes and 3.65–3.85 V along the same n-electrodes at 1 mA (scanning step: 50 mV). The forward voltage almost does not change along the same p-electrode, but it is steadily increasing along the n-electrode from top to bottom.

FIGURE 5 I-V characteristics of subpixels along (A) the same p-electrode in the row and (B) the same n-electrode in the column



The phenomenon is explained by the different resistances along the p and n electrodes: The p-electrodes are metal stacks with thick Ti/Cu whereas the n-electrodes are thin Ti/Al/Ti/Au. In this row-scan passive-matrix driving scheme, highly conductive p-electrodes are extremely desirable to reduce the voltage drop in the same row, considering that the high injection current of all 120 subpixels (dozens of microamperes) passes through one p-electrode.

Figure 6 illustrates the emission of the RGB subpixels. The EL spectra at 1 mA are plotted in Figure 6A. Photos of the RGB subpixels are given in the insets to provide an intuitive view. The emission is uniform without significant optical crosstalk around the subpixels. The peak wavelengths of the RGB subpixels are 621, 524, and 445 nm, respectively. The power of the undesired emission peaks is less than 20% of the total LOP. Relatively pure color emission is realized compared with Figure 1C (for blue/green subpixels) and Figure 4D (for red subpixels), which have no CF array coating. The CIE 1931 coordinates of the RGB subpixels are respectively indicated in Figure 6B. Our work has a comparable color gamut to sRGB, but the green and red color coordinates are shifted to the center because of the leaking blue light. It is possible to achieve wider color gamut by applying

thicker CFs or improving the LOP of green and red. A longer green emission wavelength (~ 550 nm) will also improve color mixing in the yellow-orange range, which is easy to demonstrate by tuning the epilayer growth parameters.

Optical crosstalk is an essential issue to be well addressed, especially in full-color microdisplays with color converters. The light channeling phenomenon in the sapphire substrate contributes to most of the crosstalk²⁹ rather than sidewall leakage, because the thickness of the sapphire substrate (~ 450 μm) and the emission area ($36 \mu\text{m} \times 116 \mu\text{m}$) are much greater than the height of the sidewall ($< 5 \mu\text{m}$). The crosstalk severely deteriorates the color gamut, and thus, a thick red CF layer was coated on the backside of the sapphire as an absorber²⁹ to suppress the crosstalk. A comparison of the lit-up red subpixel with and without a backside CF is demonstrated in Figure 7A,B as an example, where the photos were captured under the same conditions. The light intensity along the dashed lines is plotted in Figure 7C. Crosstalk light intensity is significantly reduced by almost one order via this approach. To further suppress the crosstalk, the ultimate solution is transferring LED pixels to other opaque or reflective substrates and removing the sapphire substrate.

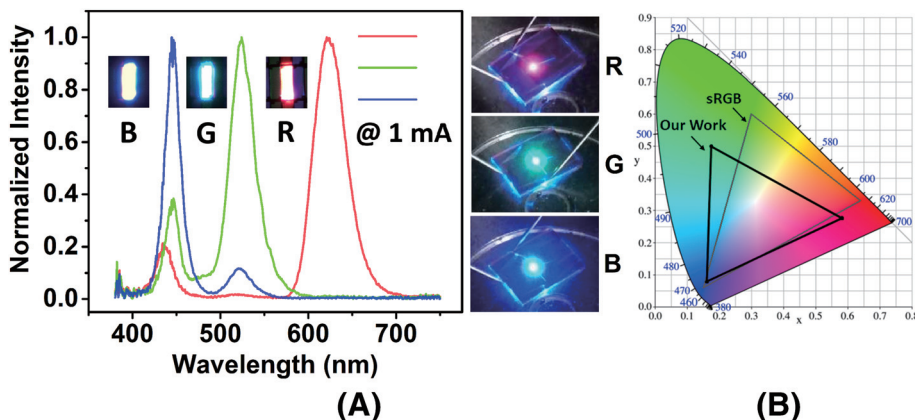


FIGURE 6 (A) EL spectra of RGB subpixels with CF. Inset: Photos of RGB subpixels. (B) CIE 1931 chromaticity diagram of RGB subpixels

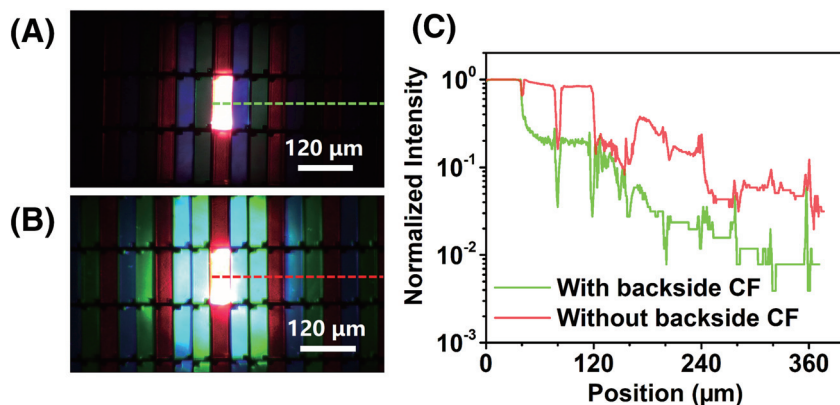


FIGURE 7 Photos of lit-up single red subpixel (A) with and (B) without backside red CF coating. (C) Comparison of optical crosstalk intensity along dashed lines

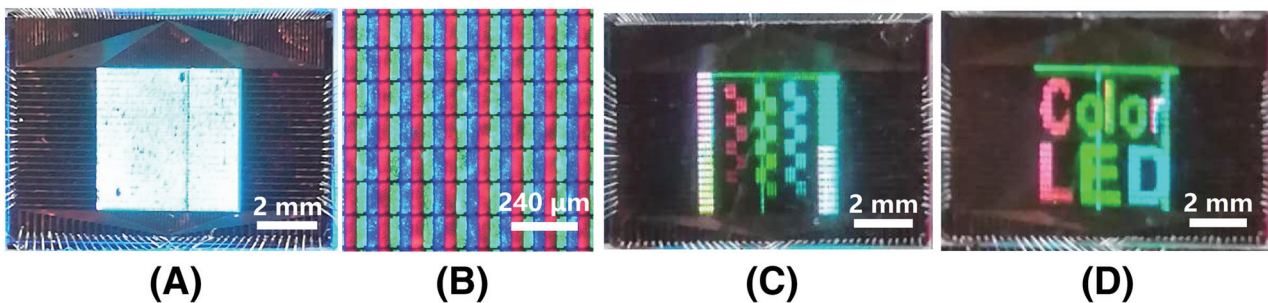


FIGURE 8 Display demo: (A) fully lit-up display panel, (B) fully lit-up RGB subpixels, (C) RGB with different grayscales and color mixing, and (D) scrolling colored text

The monolithic full-color microdisplay was driven by a full-color microdisplay controller. The controller is based on an application-specific integrated circuit (ASIC) chip that was reported by us in a previous publication.³⁰ Five series-connected shift registers are applied to provide a row scan signal to the p-electrodes. Current programmable LED driving chips serve as sink drivers for data signal input. The driving current for each subpixel is set to 1 mA by an external reference resistor. The microdisplay controller generates a pulse width modulation (PWM) signal to perform grayscale control. The demo pictures are shown in Figure 8: the fully lit-up display in Figure 8A (the whole display panel) and Figure 8B (a zoomed-in part of the display); RGB with grayscale changes and pink/cyan/yellow/white color mixing in Figure 8C; and scrolling colored text in Figure 8D. The temperature of the display panel was close to the ambient temperature, and there was no evident degradation of the QD photoresist during the operation. The pixel yield is acceptable (>90%) but is limited by our experiment instruments and could be further improved under better experimental conditions.

4 | CONCLUSION

In this work, a new approach has been invented to realize a monolithic InGaN-based LED full-color microdisplay. A passive-matrix full-color microdisplay was monolithically fabricated on blue/green dual-wavelength InGaN LED epilayers, which consists of 40×40 pixels, and each pixel includes RGB subpixels with a pitch size of $40 \mu\text{m} \times 120 \mu\text{m}$. Red QD photoresist was synthesized by mixing a QD-toluene solution and a highly transparent overcoat photoresist and then patterned on the red subpixels as a color conversion layer. A 3.5-μm-thick QD layer was finely patterned to provide efficient and uniform PL emission. Relatively pure color emission is achieved by a stripe arranged RGB CF array on the subpixels. Measurement and analysis prove that the full-

color microdisplay has a consistent forward voltage, limited optical crosstalk, and wide color gamut. Full-color images were demonstrated on the microdisplay driven by an ASIC chip-based controller, intuitively revealing the tremendous potential of this promising approach for full-color microdisplay applications in the near future.

ACKNOWLEDGEMENT

The project was supported by Innovation and Technology Support Program of Hong Kong (Project No. ITS/382/17FP).

ORCID

- Peian Li <https://orcid.org/0000-0002-2477-2844>
- Xu Zhang <https://orcid.org/0000-0001-9501-2079>
- Yangfeng Li <https://orcid.org/0000-0001-9896-9116>
- Longheng Qi <https://orcid.org/0000-0002-1012-5697>
- Chak Wah Tang <https://orcid.org/0000-0003-3135-2773>
- Kei May Lau <https://orcid.org/0000-0002-7713-1928>

REFERENCES

- Parikh K, Zhuang J, Pallister K, Jiang J, Smith M. 40-1: invited paper: next generation virtual reality displays: challenges and opportunities. SID Int Symp Dig Tec. 2018;49(1):502–505.
- Li C, Lu S, Lin S, Hsieh T, Wang K, Kuo W. 51-4: invited paper: ultra-fast moving-picture response-time LCD for virtual reality application. SID Int Symp Dig Tec. 2018;49(1):678–680.
- Ghosh A, Donoghue EP, Khayrullin I, et al. 62-1: invited paper: directly patterned 2645 PPI full color OLED microdisplay for head mounted wearables. SID Int Symp Dig Tec. 2016;47(1):837–840.
- Wu T, Sher C, Lin Y, et al. Mini-LED and micro-LED: promising candidates for the next generation display technology. Appl Sci. 2018;8(9):1557.
- Zhou X, Tian P, Sher C, et al. Growth, transfer printing and colour conversion techniques towards full-colour micro-LED display. Prog Quant Electron. 2020;71:100263.
- Wang R, Nguyen HPT, Connie AT, Lee J, Shih I, Mi Z. Color-tunable, phosphor-free InGaN nanowire light-emitting diode arrays monolithically integrated on silicon. Opt Express. 2014;22(S7):A1768–A1775.

7. Ra Y, Wang R, Woo SY, et al. Full-color single nanowire pixels for projection displays. *Nano Lett.* 2016;16(7):4608–4615.
8. Chung K, Sui J, Demory B, Teng C, Ku P. Monolithic integration of individually addressable light-emitting diode color pixels. *Appl Phys Lett.* 2017;110(11):111103.
9. Chung K, Sui J, Demory B, Ku P. Color mixing from monolithically integrated InGaN-based light-emitting diodes by local strain engineering. *Appl Phys Lett.* 2017;111(4):41101.
10. Huang Chen S, Shen C, Wu T, et al. Full-color monolithic hybrid quantum dot nanoring micro light-emitting diodes with improved efficiency using atomic layer deposition and non-radiative resonant energy transfer. *Photonics Res.* 2019;7(4):416.
11. Cheung YF, Choi HW. Color-tunable and phosphor-free white-light multilayered light-emitting diodes. *IEEE T Electron Dev.* 2013;60(1):333–338.
12. Kang C, Kong D, Shim J, et al. Fabrication of a vertically-stacked passive-matrix micro-LED array structure for a dual color display. *Opt Express.* 2017;25(3):2489.
13. Kang C, Kang S, Mun S, et al. Monolithic integration of AlGaInP-based red and InGaN-based green LEDs via adhesive bonding for multicolor emission. *Sci Rep.* 2017;7(1):10333.
14. Kang C, Lee J, Kong D, et al. Hybrid full-color inorganic light-emitting diodes integrated on a single wafer using selective area growth and adhesive bonding. *ACS Photonics.* 2018;5(11):4413–4422.
15. Liu Z, Lin C, Hyun B, et al. Micro-light-emitting diodes with quantum dots in display technology. *Light Sci Appl.* 2020;9(1):83.
16. Han H, Lin H, Lin C, et al. Resonant-enhanced full-color emission of quantum-dot-based micro LED display technology. *Opt Express.* 2015;23(25):32504–32515.
17. Lin HY, Sher CW, Hsieh DH, et al. Optical cross-talk reduction in a quantum-dot-based full-color micro-light-emitting-diode display by a lithographic-fabricated photoresist mold. *Photonics Res.* 2017;5:411–416.
18. Park J, Kyhm J, Kim HH, et al. Alternative patterning process for realization of large-area, full-color, active quantum dot display. *Nano Lett.* 2016;16(11):6946–6953.
19. Ji T, Jin S, Zhang H, Chen S, Sun XW. Full color quantum dot light-emitting diodes patterned by photolithography technology. *J Soc Inf Display.* 2018;26(3):121–127.
20. Kim HJ, Shin MH, Hong HG, et al. Enhancement of optical efficiency in white OLED display using the patterned photoresist film dispersed with quantum dot nanocrystals. *J Disp Technol.* 2016;12(6):526–531.
21. Lee E, Kan S, Hotz C, et al. 67-2: invited paper: ambient processing of quantum dot photoresist for emissive displays. *SID Int Symp Dig Tec.* 2017;48(1):984–987.
22. Kim H, Ryu M, Cha JHJ, Kim HS, Jeong T, Jang J. Ten micrometer pixel, quantum dots color conversion layer for high resolution and full color active matrix micro-LED display. *J Soc Inf Display.* 2019;27(6):347–353.
23. Qi YD, Liang H, Tang W, Lu ZD, Lau KM. Dual wavelength InGaN/GaN multi-quantum well LEDs grown by metalorganic vapor phase epitaxy. *J Cryst Growth.* 2004;272(1):333–340.
24. Lin WH, Chang SJ, Chen WS. GaN-based dual-color light-emitting diodes with a hybrid tunnel junction structure. *J Disp Technol.* 2016;12(2):165–170.
25. Jiang Y, Li Y, Li Y, et al. Realization of high-luminous-efficiency InGaN light-emitting diodes in the “green gap” range. *Sci Rep.* 2015;5:10883.
26. Kisim M, Mamedov D, El-Ghoroury H. Simulation of full-color III-nitride LED with intermediate carrier blocking layers. *Opt Quant Electron.* 2016;48(12):1–9.
27. Hong Q, Lee K, Luo Z, Wu S. High-efficiency quantum dot remote phosphor film. *Appl Optics.* 2015;54(15):4617–4622.
28. Moon H, Lee C, Lee W, Kim J, Chae H. Stability of quantum dots, quantum dot films, and quantum dot light-emitting diodes for display applications. *Adv Mater.* 2019;31(34):1804294.
29. Li KH, Cheung YF, Tang CW, Zhao C, Lau KM, Choi HW. Optical crosstalk analysis of micro-pixelated GaN-based light-emitting diodes on sapphire and Si substrates. *Phys Status Solidi a.* 2016;213(5):1193–1198.
30. Chong WC, Cho WK, Liu ZJ, Wang CH, Lau KM. Pixels per inch (PPI) passive-matrix micro-LED display powered by ASIC. *CSICS.* 1700;2014:1–4.

AUTHOR BIOGRAPHIES



Peian Li received the Bachelor of Science (BS) degree in chemistry from Tsinghua University, Beijing, China, in 2017. He is currently a Doctor of Philosophy (PhD) candidate in the Department of Electronic and Computer Engineering, Hong Kong University of Science and Technology, Hong Kong. His research interests include GaN-based LEDs and LED microdisplays.

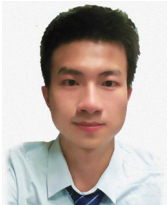


Xu Zhang received the BS degree in microelectronic science from the University of Electronic Science and Technology of China, Sichuan, China, in 2014, and the PhD degree in electronic and computer engineering from Hong Kong University of Science and Technology, Hong Kong, in 2019. He is currently a postdoctoral fellow in the Department of Electronic and Computer Engineering, Hong Kong University of Science and Technology, Hong Kong. His research interests include GaN-based vertical devices and LED microdisplays.



Yangfeng Li received the BS degree in material physics from Wuhan University, Hubei, China, in 2012, and the PhD degree in condensed matter physics from the Institute of Physics, University of Chinese Academy of Sciences, Beijing, China, in

2018. He was a postdoctoral fellow in the Department of Electronic and Computer Engineering, Hong Kong University of Science and Technology, Hong Kong, from 2018 to 2019. He is currently a postdoctoral fellow in the Institute of Physics, Chinese Academy of Sciences, Beijing, China. His research interests include III-nitride epitaxy growth and GaN-based devices.



Longheng Qi received the Bachelor of Engineering (B.Eng.) degree in electronic science and technology from the University of Electronic Science and Technology of China, Sichuan, China, in 2018. He is currently a PhD candidate in the Department of Electronic and Computer Engineering, Hong Kong University of Science and Technology, Hong Kong. His research interest is full-color LED microdisplays.



Chak Wah Tang received the Master of Science (MS) degree in electrical engineering from Taiwan National Cheng Kung University, Tainan, Taiwan, in 1996. He is currently a Senior Technical Officer in the Department of Electronic and Computer Engineering, Hong Kong, University of Science and Technology, Hong Kong. His research interests include III-nitride and III-V material growth, development, and characterization.



Kei May Lau is the Fang Professor of Engineering at the Hong Kong University of Science and Technology (HKUST). She received the BS and MS degrees in physics from the University of Minnesota, Minneapolis, and the PhD degree in Electrical Engineering from Rice University, Houston, Texas. She was on the ECE faculty at the University of Massachusetts/Amherst and initiated MOCVD, compound semiconductor material, and device programs. Since the fall of 2000, she has been with the ECE Department at HKUST. She established the Photonics Technology Center for R&D effort in III-V materials, optoelectronic, high power, and high-speed devices. Professor Lau is a Fellow of the Hong Kong Academy of Engineering Sciences, IEEE, and OSA, a recipient of the US National Science Foundation (NSF) Faculty Awards for Women (FAW) Scientists and Engineers (1991), Croucher Senior Research Fellowship (2008), and the IEEE Photonics Society Aron Kressel Award (2017) and OSA Nick Holonyak Award (2020). She was an Editor of the IEEE TED, EDL, Applied Physics Letters, and Journal of Crystal Growth.

How to cite this article: Li P, Zhang X, Li Y, Qi L, Tang CW, Lau KM. Monolithic full-color microdisplay using patterned quantum dot photoresist on dual-wavelength LED epilayers. *J Soc Inf Display*. 2020;1–9. <https://doi.org/10.1002/jsid.966>